Journal of Nuclear Materials 386–388 (2009) 716–719

Contents lists available at ScienceDirect

Journal of Nuclear Materials

journal homepage: www.elsevier.com/locate/jnucmat

Fluoridation and oxidation characteristics of JLF-1 and NIFS-HEAT-2 low-activation structural materials

Takuya Nagasaka [a,*], Masatoshi Kondo [a], Takeo Muroga [a], Nobuaki Noda [a], Akio Sagara [a], Osamu Motojima [a], Akihiro Suzuki [b], Takayuki Terai [c]

[a] National Institute for Fusion Science, Oroshi 322-6, Toki, Gifu 509-5292, Japan
[b] Nuclear Professional School, Graduate School of Engineering, The University of Tokyo, 2-22 Shirakata-Shirane, Tokai, Naka, Ibaraki 319-1188, Japan
[c] Department of Nuclear Engineering and Management, Graduate School of Engineering, The University of Tokyo, 7-3-1 Hongo, Bunkyo-ku, Tokyo 113-8656, Japan

A B S T R A C T

Fluoridation and oxidation of JLF-1 (Fe–9Cr–2W–0.1C) and NIFS-HEAT-2 (V–4Cr–4Ti) were examined under various corrosion conditions, such as Flibe ($2LiF + BeF_2$) molten salt at 823 K for 2003 h, H_2O–47%HF solution at RT for 2 min, and He–(0–1%)HF gas mixture containing moisture and O_2 gas impurities at 823 K for 2.5–100 h. Oxidation dominated fluoridation under all test conditions, even when the fluoridation agent, the F atoms in HF, was 16× more plentiful than the oxidation agent, O atoms in H_2O, and O_2. Corrosion products were mainly considered as Cr_2O_3, while fluoride was indicated in a very limited surface region. JLF-1 exhibited better corrosion resistance in He–HF gas mixture tests than NIFS-HEAT-2.

1. Introduction

Reduced-activation ferritic steels (RAF, Fe–(8–9)Cr–(1–2)W–0.1C steels) and low-activation vanadium alloys (V–4Cr–4Ti) are candidate structural materials for a fusion blanket [1,2]. Flibe ($LiF + BeF_2$) is an attractive breeding material for an advanced fusion blanket system [3]. Corrosion of structural materials received most attention in Flibe blanket development. Possible corrosion agents in Flibe are HF, H_2O, O_2 and metal impurities. In order to clarify the corrosion mechanism in Flibe, it is essential to understand the competitive processes of fluoridation and oxidation. This study seeks to characterize corrosion products of the low-activation materials after fluoridation, oxidation and Flibe exposure tests, and to evaluate corrosion resistance of the low-activation materials in Flibe conditions.

2. Experimental procedure

The low-activation materials used were one-inch-thick plates of JLF-1 JOYO-II heat (Fe–9.00Cr–1.98W–0.090C–0.015N–0.20V–0.083Ta) and NIFS-HEAT-2 (NH2, V–4.02Cr–3.98Ti–0.0069C–0.0122N–0.0148O). One-millimeter-thick plates of pure metal (99.9–99.99%) of Fe, Cr, W, Ni, V and Ti were also prepared. The annealing conditions for JLF-1 were normalizing at 1323 K for 1 h, and air cooling and tempering at 1053 K for 1 h. The final annealing for NH2 and the pure metals was 1273 K for 2 h and 1 h, respectively. Coupon specimens with sizes of $10 \times 20 \times 1$ mm or $10 \times 15 \times 1$ mm were machined from the plates. The specimen surface average roughness was 2 μm.

The specimens were exposed to Flibe ($2LiF + BeF_2$) molten salt at 823 K for 2003 h, H_2O–47%HF solution at room temperature (RT) for 2 min and He–(0–1%)HF gas mixture (He–*x*HF) at 823 K for 2.5–100 h. He gas contained moisture (H_2O) and O_2 as impurities. The moisture and O_2 concentrations were, respectively, measured with a dewpoint transmitter XDT-PM-PB (Xentaur) and an oxygen analyzer DF-150 (Delta F Co.). HF gas was generated by reaction between H_2 gas and NiF_2 at 873 K. The HF concentration was determined by titration. Table 1 lists He–*x*HF gas compositions. H_2O and O_2 concentrations in He–0.1%HF and He–1%HF were evaluated before HF generation, since the gas analyzers cannot be used for corrosive gas.

The weight change of the exposed specimens was measured. The specimen surface was analyzed by scanning electron microscope (SEM) and X-ray photoelectron spectrometry (XPS). The specimen exposed to Flibe was cleaned with LiCl–KCl molten salt mixture to remove Flibe before the analyses.

3. Results

Fig. 1 plots the weight change after the corrosion tests. Weight loss of pure Ni was negligible in H_2O–47%HF solution. The low-activation materials, JLF-1 and NH2, exhibited similar weight losses, which were comparable to the base metals, V and Fe. Cr and W exhibited a 1/30–1/50 weight loss compared with the low-activation materials. The weight gain of NH2 in the He–*x*HF gas mixture was 10–30× greater than that of JLF-1. The weight gain of JLF-1 in He–1%HF was greater than that in He–0.1%HF,

* Corresponding author. Tel.: +81 572 58 2252; fax: +81 572 58 2676.
E-mail address: nagasaka@nifs.ac.jp (T. Nagasaka).

0022-3115/$ - see front matter © 2009 Elsevier B.V. All rights reserved.
doi:10.1016/j.jnucmat.2008.12.296

Table 1
Gas composition of He–HF gas mixture. F/O indicates the ratio of the number of F atoms to O atoms in the gas mixture.

Nominal composition	H_2O (%)	O_2 (%)	HF (%)	F/O
He	0.0027	0.0089	–	0
He–0.1%HF	0.055[a]	0.0016[a]	0.14[b]	2.4
			0.16[c]	2.7
He–1%HF	0.055[a]	0.0016[a]	0.96[b]	16
			0.92[c]	16

[a] Before HF generation.
[b] For JLF-1 specimen.
[c] For NH2 specimen.

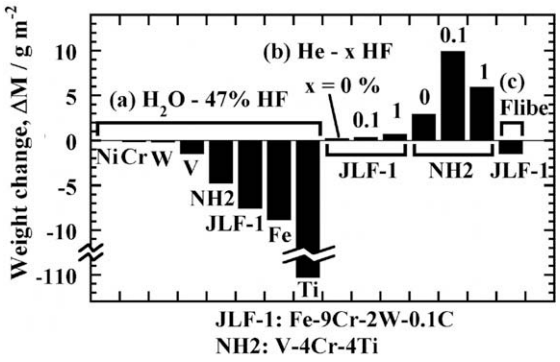

Fig. 1. Weight change after corrosion tests. Corrosion conditions were: (a) RT × 2 min, (b) 823 K × 100 h for He, 25 h for He–0.1%HF, 2.5 h for He–1%HF, and (c) 823 K × 2003 h.

while a lesser weight gain was observed for NH2 in He–1%HF than in He–0.1%HF. In contrast, JLF-1 exhibited weight loss in Flibe.

Fig. 2 presents SEM images of the specimen surface before and after the corrosion tests. Particles with various sizes under 1 μm were observed. The number density of the particles for NH2 was higher than that of JLF-1. The particles coalesced in NH2.

The composition of corrosion products on the surface was analyzed by XPS with Ar sputtering. Fig. 3 depicts the typical depth profiles for composition. The sputtering rate was 4.87 nm/min in SiO_2 and was not significantly different from other materials, so that 30 min sputtering should be equivalent to about 150 nm in depth from the surface. In all specimens, the intensity of photoelectrons from O atoms was much higher than that from F atoms, even when there were 16× more F atoms than O atoms in the He–1%HF atmosphere (indicated in Table 1 as F/O = 16). At the peak of F atoms in Fig. 3(a) for the Flibe condition, the ratio of F/O was calculated to be 0.25 using atomic sensitivity factors for X-ray. The F/O ratio of JLF-1 after exposure to H_2O–47%HF solution was 3.6 at the surface before Ar sputtering, and was 0.6 after 10 min sputtering. After NH2 exposure to the HF solution, F/O was 0.39 at the surface and 0.20 after 10 min of Ar sputtering. For exposure to the He–HF gas mixture, F/O was <0.36 for both JLF-1 and NH2 at all HF concentrations. The F/O ratio indicated that fluoridation occurred much less than oxidation except for JLF-1 after exposure to the H_2O–HF solution. Analyses by XPS also indicated that fluoridation was very limited in the surface. Fluoridation depth was estimated to be 10 nm to <100 nm at the maximum, whereas oxidation was detected at more than 100 nm.

XPS (Fig. 3) revealed that Cr was segregated at the surface of JLF-1 in He–(0–1%)HF gas, and at the surface of NH_2 in He–1%HF gas. In order to investigate the binding of Cr atoms in the corrosion products, the photoelectron energy spectrum around the peaks of the 2p electron in Cr were compared to pure Cr (99.9% purity) and Cr_2O_3 (99.9%). Fig. 4 summarizes the comparisons. 2p Photoelectron spectra of the JLF-1 and NH_2 before exposure were close to that of pure Cr (Fig. 4(a)1 and (b)1). Therefore, Cr was in a metal state in both alloys. In contrast, the spectra for JLF-1 under He–(0–1%)HF conditions and NH_2 under He–(0.1%, 1%)HF conditions were similar to those of Cr_2O_3 (Fig. 4(a)4, 5, 6 and (b)5, 6). The other conditions for JLF-1 yielded different positions of 2p photoelectron peaks, which seemed to shift toward higher energy (Fig. 4(a)2, 3). The other conditions for NH_2 produce no peaks in the analyzed energy area (Fig. 4(b)2, 4).

4. Discussion

4.1. Competition between fluoridation and oxidation

For two low-activation materials, JLF-1 and NH2, oxidation was dominant under He–(0–1%)HF gas conditions, even if the fluorida-

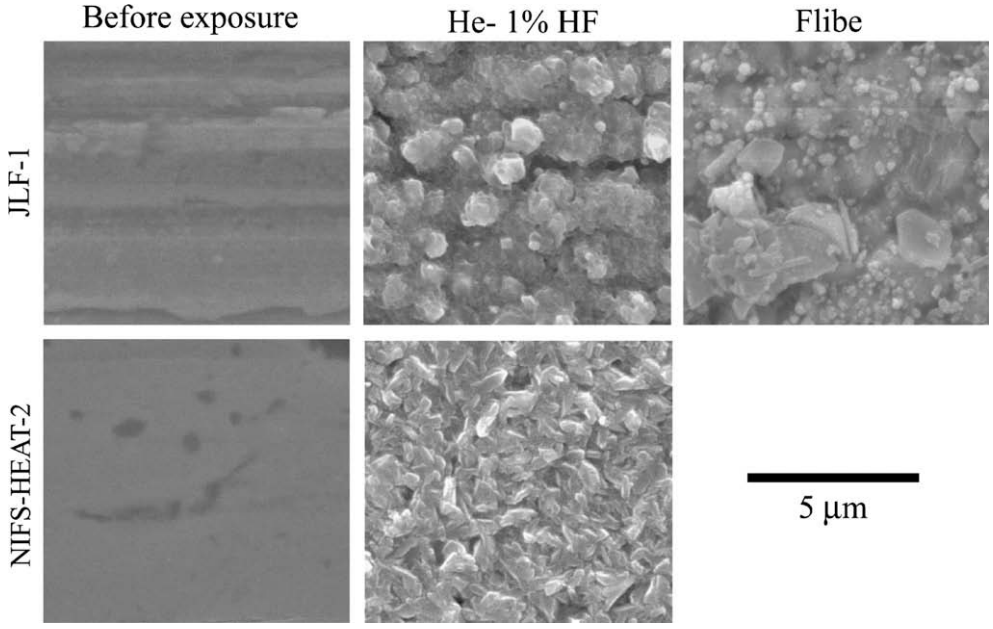

Fig. 2. SEM images of the surface before and after corrosion tests.

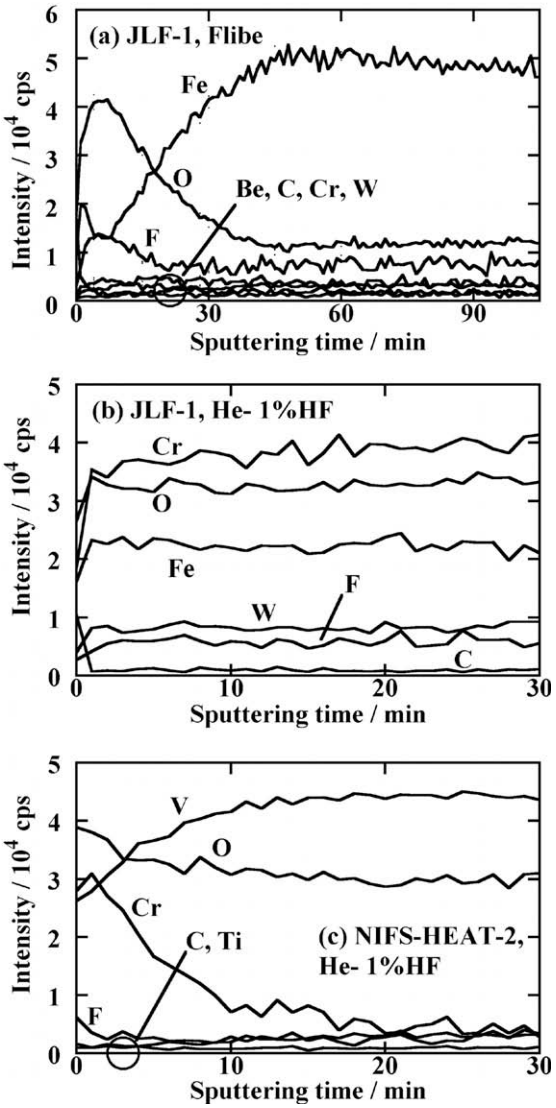

Fig. 3. Depth profile of photoelectron intensity. Sputtering rate was 4.87 nm in SiO_2.

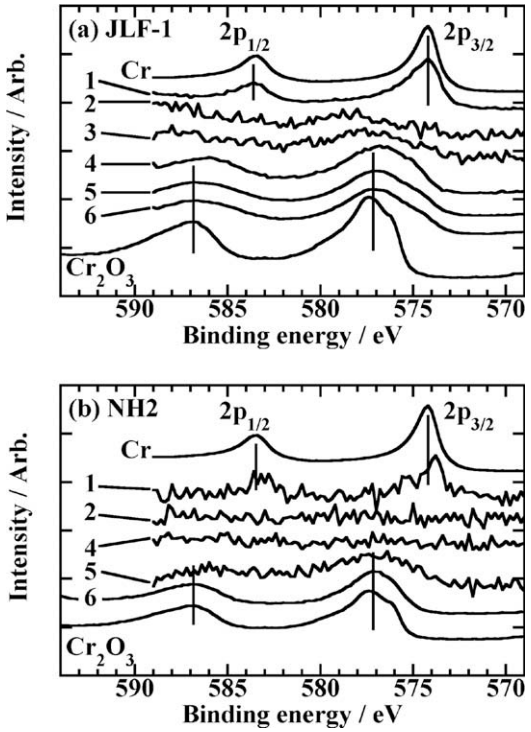

Fig. 4. Comparison of 2p photoelectron spectra among pure Cr, Cr_2O_3, and Cr on the surface of: (a) JLF-1 and (b) NH2 before and after the corrosion tests. Corrosion conditions are as follows: (1) before exposure. (2) H_2O–47%HF. (3) Flibe. (4) He. (5) He–0.1%HF. (6) He–1%HF. Spectra for the corrosion products were acquired at the maximum point for F atoms in the depth profile of compositions. Spectra are intensified to see the peak more easily, with intensification factors differing for each spectrum.

tion agent, F atom in HF, was 16× more numerous than oxidation agents, O atom in H_2O and O_2. Stable phase equilibria calculated for a Flibe-Fe–9Cr–2W system and a Flibe-V–4Cr–4Ti system in an Ar atmosphere including O_2 and HF gases [4]. Cr_2O_3 was predicted when H_2O addition was as high as 0.1% in the Ar gas, and then Fe-Cr_2O_4 became dominant above 1% in the Flibe-Fe–9Cr–2W system. Furthermore, CrF_2 was formed when 0.1%HF was added, while CrF_3 appeared at around 1%HF. The binding energy in Fig. 4(a) indicated Cr(III) for He–(0–1%)HF gas conditions. Cr_2O_3 and CrF_3 are possible, however, the main compound of the corrosion products is considered to be Cr_2O_3, since Fig. 3(b) indicated a much higher Cr concentration than F concentration. In contrast, 2p photoelectron peaks of Cr after exposure to HF–47%HF and Flibe differed from both the metal Cr and Cr(III). Moreover, the Fe concentration was higher than Cr in Flibe condition (Fig. 3(a)). Thus, other compounds should be taken into account. MF_2 (M = Fe, Cr) is possible considering the stable phase equilibria mentioned above. Moreover, MF_3 type is still possible, since binding energies of 2p photoelectrons in $Cr(III)F_3$ may differ from $Cr(III)_2O_3$. Standard photoelectron spectra were not available for these fluorides, which will be taken in the near future, and are yet to be identified. Small angle X-ray diffractometry (XRD) in a previous study has indicated FeF_2 and CrF_2 as well as oxides including Li, Fe, and Be [5].

Oxidation was also dominant in NH2. Therefore, the lower weight gain under He–1%HF conditions than under He–0.1%HF conditions in Fig. 1 is caused by a shorter corrosion test time, which means the total O supply is less. Fig. 3(c) depicts Cr segregation, and Fig. 4(b) indicates Cr_2O_3 formation in corrosion products on NH2. These are surprising because NH2 contains Ti, which is known to form very stable oxide in vanadium alloys [6]. More TiO should form than Cr_2O_3 because Gibbs formation free energy of TiO at 823 K is -461 kJ mol^{-1} per O atom, whereas that of Cr_2O_3 is -306 kJ mol^{-1} per O atom. Stable phase equilibria calculation has also indicated TiO under 0.1%H_2O conditions, or TiF_3 under 0.1%HF conditions [4]. The present experiment results suggest that gas compounds, such as TiF_2 (-353 kJ mol^{-1} per F atom), might be formed before the most stable compound, TiF_3 (-412 kJ mol^{-1} per F atom), and that Ti was then lost by evaporation of TiF_2 into the gas atmosphere.

4.2. Corrosion resistance to Flibe condition

The fundamental process of weight loss in Flibe is considered to be formation of corrosion products in He or He–xHF gas and their dissolution into Flibe. In the gas conditions depicted in Fig. 1, specimens gained weight because all the corrosion products remained on the specimen surface. In contrast, samples lost weight under Flibe conditions because the corrosion products were partly lost by dissolution into Flibe. He–xHF gas conditions are thought to be accelerated tests for corrosion product formation under Flibe conditions.

Under fusion conditions, tritium (T) is generated in Flibe by the breeding reaction between Li and neutrons and forms TF, which is chemically equivalent to a corrosion agent such as HF. Generation of TF in a helical fusion power reactor (FFHR) has been estimated to

be 0.0030% per day [7]. Pettie et al. simulated this continuous HF generation [8]. Surface analyses of JLF-1 after Flibe exposure have also revealed oxidation-dominant corrosion, such as the formation of Cr_2O_3 [9]. Under fusion-reactor conditions, the oxygen impurity concentration is probably low, therefore the fraction of fluoridation should be increased. Oxygen and fluorine must be systematically controlled, especially to lower oxygen concentration for the corrosion test to simulate and predict corrosion under fusion-reactor conditions.

The weight loss of JLF-1 after Flibe exposure at 823 K for 2003 h (1.5 g m^{-2}, Fig. 1) was not significant because it is less than the 2.85 g m^{-2} obtained for type 316 stainless steel exposed to Na at 773 K, which has been established for fast-breeder reactor systems [10]. As mentioned above, the weight gain after the He–*x*HF gas corrosion test (Fig. 1) is mainly caused by oxidation. Formation of corrosion products and weight gain for NH2 was 10–30× greater than those for JLF-1. Based on these results, NH2 is thought to exhibit a one order of magnitude greater weight loss than JLF-1 under Flibe conditions, if the oxidized layer is lost in Flibe. From the corrosion view point, stricter oxygen reduction control will be required for a Flibe-vanadium alloy system.

5. Conclusions

(1) Oxidation was dominant in samples exposed to Flibe molten salt and He–0.055H_2O–0.0016O_2–(0.1%, 1%)HF gas conditions. Most of the weight change can be attributed to oxygen pickup. Corrosion products mainly consist of Cr_2O_3 in both NH2 and JLF-1.

(2) JLF-1 corrosion characteristics are considered acceptable as a blanket structural material at 823 K for 2003 h under static Flibe conditions. However, corrosion of vanadium alloy (NIFS-HEAT-2, NH2) under He–HF gas conditions was 10–30× greater than that of ferritic steel (JLF-1). From the corrosion view point, stricter oxygen reduction control will be required for a Flibe-vanadium alloy system.

Acknowledgement

This study was promoted by NIFS budget code NIFS07UCFF002.

References

[1] S. Jitsukawa et al., J. Nucl. Mater. 329–333 (2004) 39.
[2] T. Muroga et al., J. Nucl. Mater. 367-370 (2007) 780.
[3] A. Sagara et al., Fus. Eng. Des. 81 (2006) 2703.
[4] T. Terai et al., J. Nucl. Mater. 258–263 (1998) 513.
[5] T. Nagasaka, M. Kondo, H. Nishimura, T. Yakata, N. Noda, T. Muroga, A. Sagara, A. Suzuki, T. Terai, J. Nucl. Mater., submitted for publication.
[6] N.J. Heo et al., J. Nucl. Mater. 307–311 (2002) 620.
[7] H. Nishimura et al., J. Nucl. Mater. 307–311 (2002) 1355.
[8] D.A. Pettie et al., Fus. Eng. Des. 81 (2006) 1439.
[9] P. Calderoni et al., Control of molten salt corrosion of reduced activation steel for fusion application, in: 13th International Conference on Fusion Reactor Materials, 10–14 December, 2007, Nice, France.
[10] V. Ganesan et al., J. Nucl. Mater. 256 (1998) 69.